

Modeling system and data

The ensemble forecasts analyzed in this work are obtained through the atmospheric general circulation model GLOBO, a global, hydrostatic model with regular latitude-longitude grid:

- horizontal grid spacing of 0.56 deg lat x 0.8 deg lon with output (grib2 files) on 1.5° x 1.5° grid;
- 54 vertical hybrid levels, 7 soil layers;
- slab ocean simple model for sea-surface temperature (SST) evolution;
- sea-ice cover fixed if > (<) than climatology (1981–2010) in the fall-winter (spring-summer) season; relaxed to climatology otherwise. Both SST and sea-ice climatologies are computed from ECMWF ERA-Interim reanalyses.

The dataset verified here is made up of 106 forecasts operationally produced, on a weekly basis, starting on the 29 March 2015 and covering about 2 years. Each forecast is produced with the following strategy:

- mixed lagged-perturbed ensemble of 41 members;
- 32-day simulations initialized every Wednesday 4 forecasts each month;
- 10 runs at 00, 06, 12, 18 UTC of Wednesday + 1 “control” run at 00 UTC of Thursday;
- initial conditions from NOAA-NCEP GEFS forecasts at 0-h lead time (analyses).

Forecasts are calibrated with reforecast simulations initialized with data obtained from ERA-Interim reanalyses. A single run is initialized every 5 days to cover the 1981–2010 reference period, for a total of 2190 simulations. Currently, a new reforecast dataset based on a 5-member ensemble is available on the S2S database, but in this work the old reforecast dataset is used.

The forecast verification is performed against ERA-Interim reanalyses and is based on week averages starting from the first forecast day.

Deterministic scores

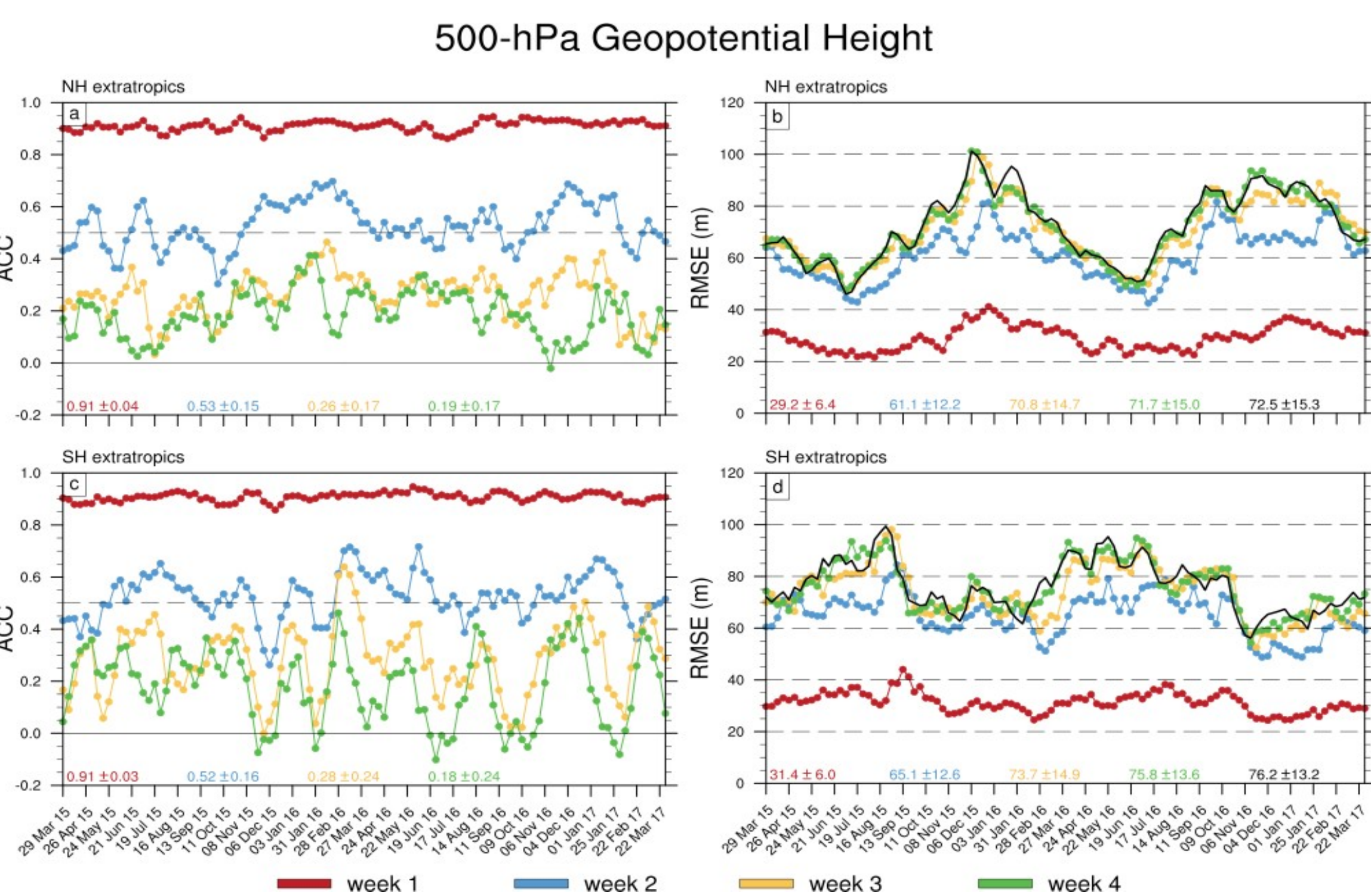


Fig. 1: Anomaly correlation coefficient (a, c) and root mean square error (b, d) of weekly means of Z500 averaged over the Northern (> 20°N, top panels) and Southern (<20°S, bottom panels) Hemisphere extratropics. The black time series in panels b and d represents the climatological RMSE. At the bottom of each panel, the mean and standard deviation of the time series with matching color are reported. A 4-point moving average has been applied to the displayed time series.

Probabilistic scores

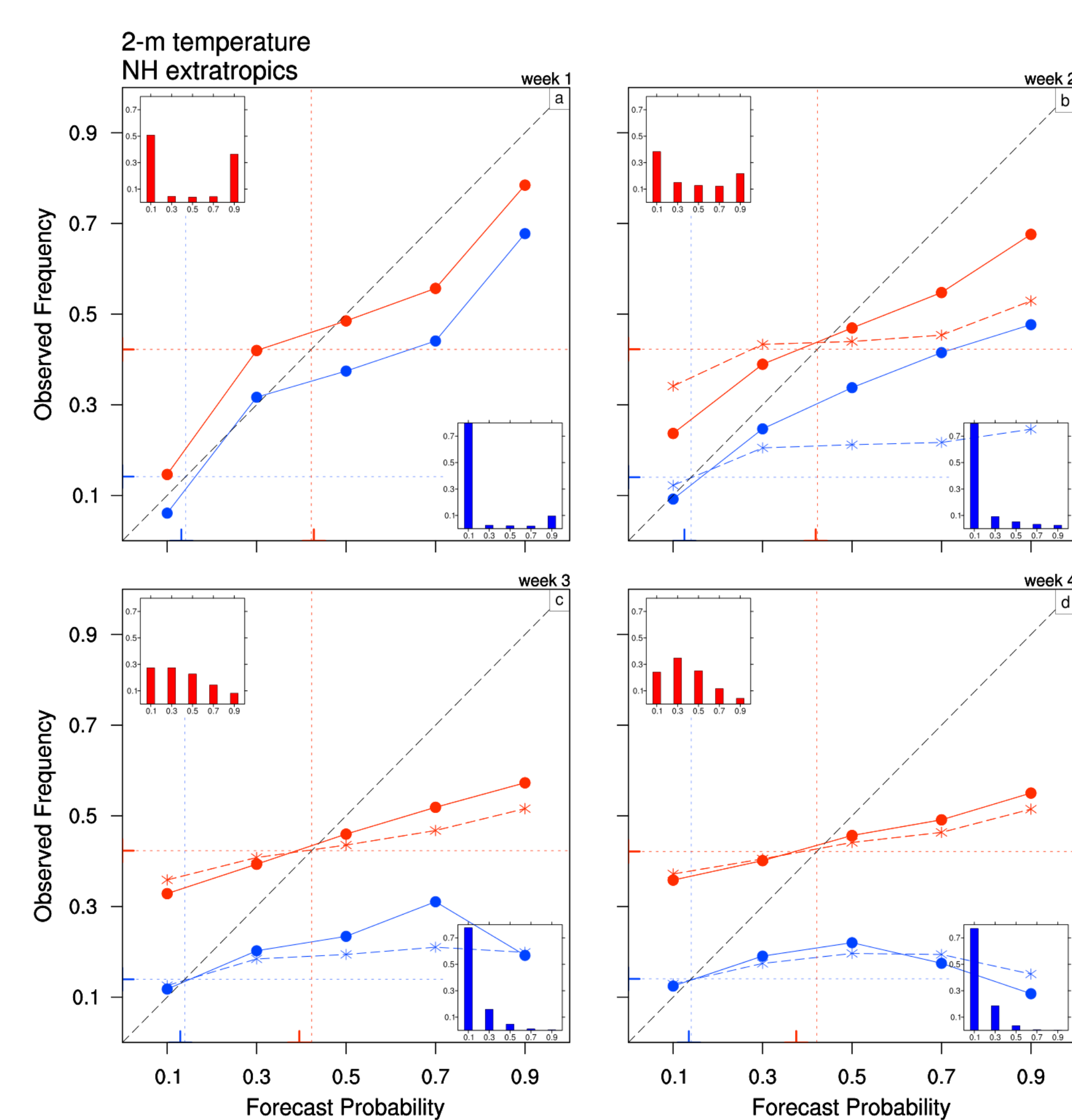


Fig. 2: Reliability diagrams computed from 106 weekly averaged T2m forecasts, over land points of the extratropical Northern Hemisphere, for week 1 (a), 2 (b), 3 (c), 4 (d). Red (blue) color refers to above-normal (below-normal) events. The histograms of the relative forecast probability frequencies are shown on the top-left (warm events) and bottom-right (cold events) corner of each panel. The dashed curves in panels b, c, d are obtained persisting the probabilities for the previous week of the same forecast. Marks on the left and bottom edge indicate the mean observed frequency and the mean forecast frequency, respectively. The dotted lines starting from the mean observed frequency marks (y axis) are drawn from both axes to indicate the no-resolution boundaries.

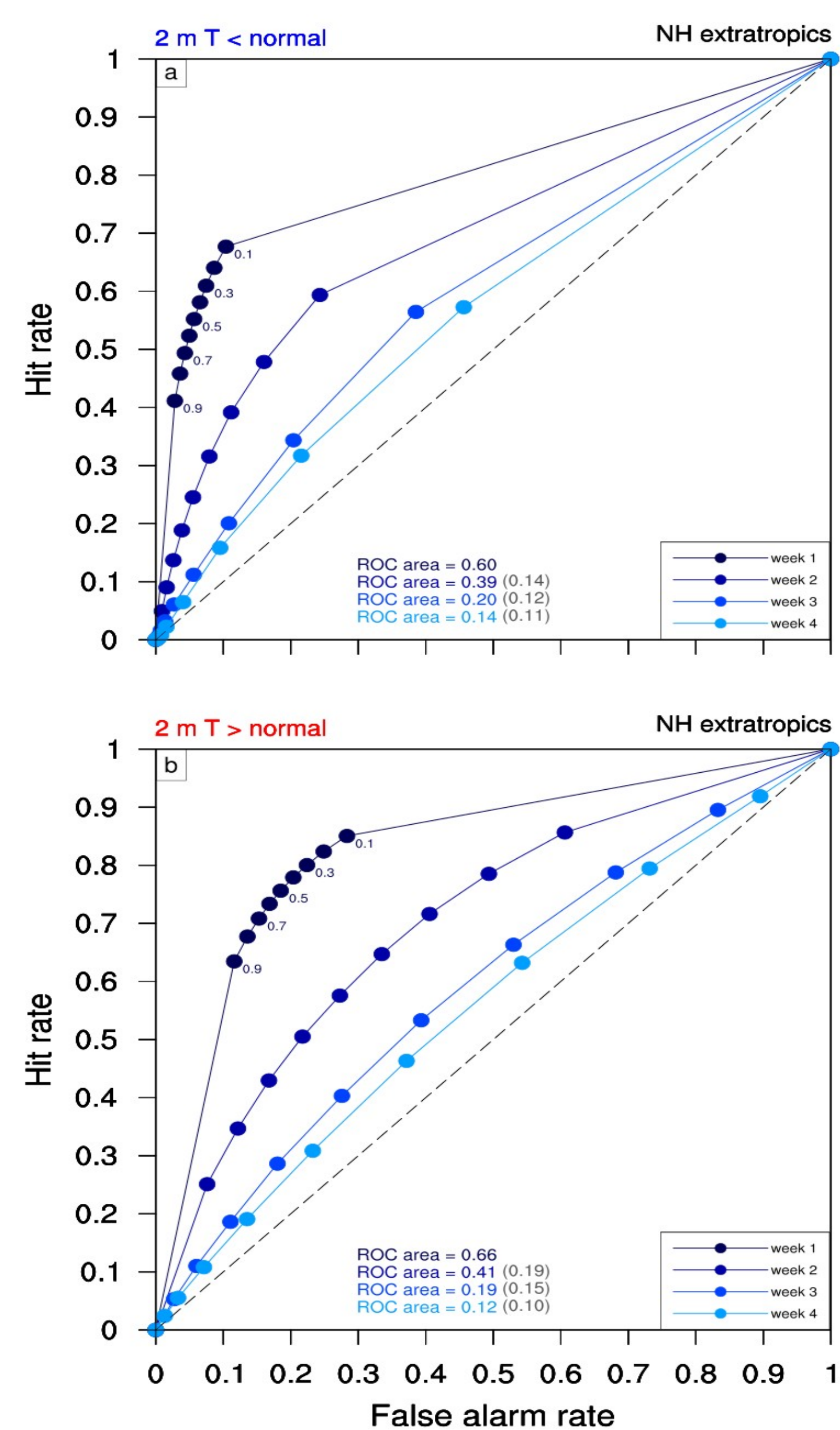


Fig. 4: ROC diagrams computed from 106 weekly averaged forecasts of T2m over land points of the extratropical Northern Hemisphere, for below-normal (a) and above-normal events (b). The area under the curve for each forecast week is reported at the bottom of each panel; the same value obtained persisting the probabilities for the previous week of the same forecast is reported in brackets for weeks 2-4.

The combination of the low value of the observed frequency of the below-normal category, together with the adopted binning interval (0.2), hinders most of the information contained in the reliability curves of cold events. To overcome this issue, a reliability diagram created through an adaptive binning based on the forecast frequency (as proposed by Brocker and Smith, 2007*) has been adopted and compared for week 3 and 4 (Fig. 3). The clustering underlying the new reliability evaluation highlights enhanced resolution for very low forecast probabilities, indicating that cold-event distribution is more confident than what suggested by the histograms in Fig.2. The new clustering has small impact on the reliability of warm-event prediction due to the greater confidence of its refinement distribution, which also implies significant occupation of all probability bins.

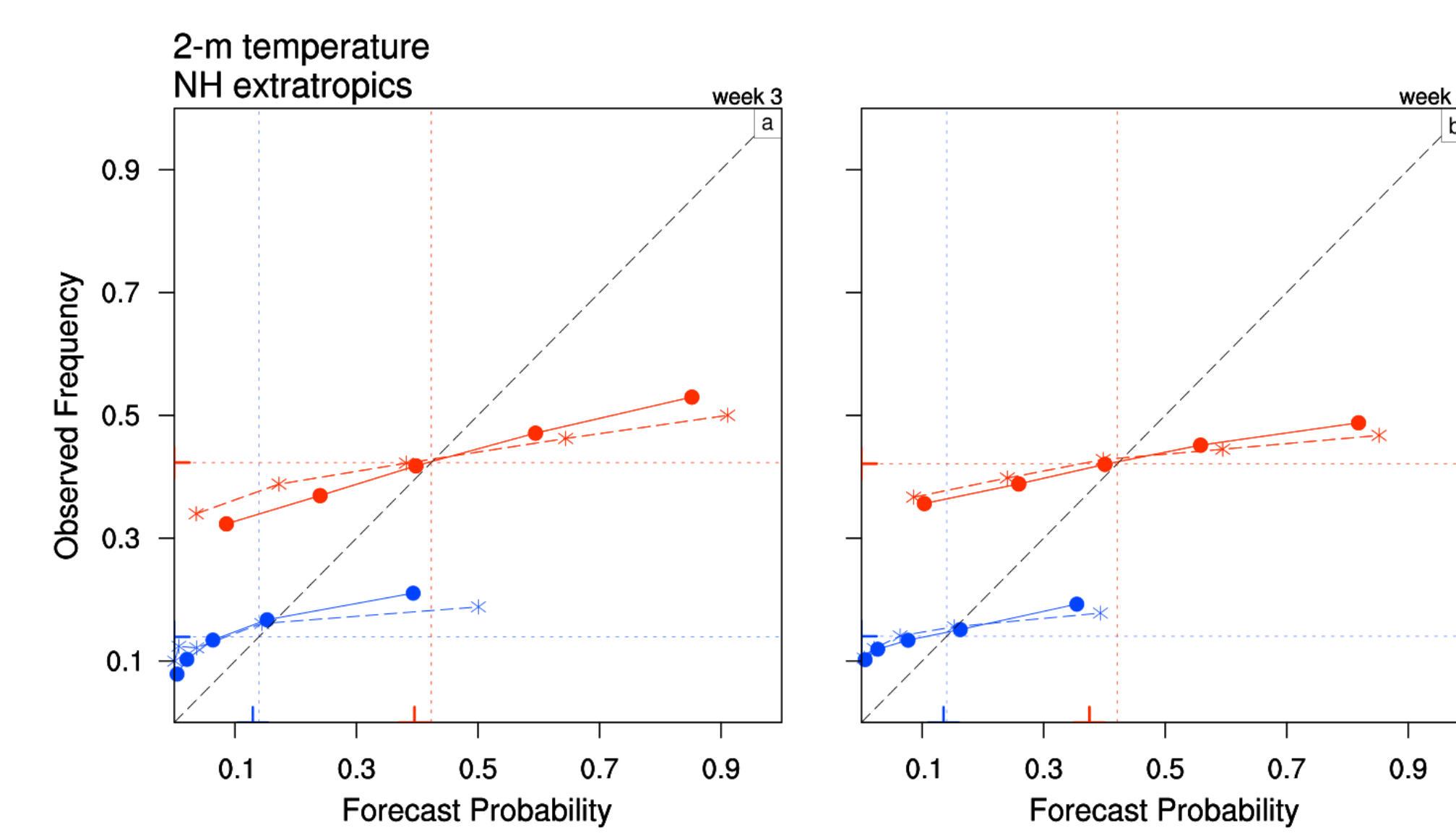


Fig. 3: As in Fig.2 but for week 3 (a) and 4 (b). The abscissa of the calibration curves show the mean forecast probability of 5 equally populated bins.

* Bröcker, J. and L.A. Smith, 2007: Increasing the Reliability of Reliability Diagrams. Wea. Forecasting, 22, 651–661, <https://doi.org/10.1175/WAF993.1>

Summary

The monthly forecasting system developed at CNR-ISAC is operationally run on a weekly basis to produce 41-member ensemble forecasts in the framework of the Subseasonal-to-Seasonal (S2S) project. In this work, two years of forecasts, covering 106 weeks from April 2015, are verified against ERA-Interim reanalyses. The evaluation is based on weekly averages starting from the first forecast day.

The anomaly correlation coefficient of 500-hPa geopotential height shows enhanced predictive skill during the cold months, when favorable values are occasionally obtained beyond week 2. The root mean square forecast error saturates towards the climatological value between week 2 and 3.

Reliability diagrams are used to evaluate the probabilistic forecast skill of 2-m temperature over Northern Hemisphere extratropical land points, in terms of above/below normal events. For each category, the forecasting system loses reliability and resolution beyond week 2, but it approximately reproduces the observed 2-year mean frequency up to week 4, resulting unconditionally unbiased. The reliability of the forecasting system systematically outperforms the reliability obtained by persisting the probabilities from the previous week of the same forecast.

Beyond week 2, the forecast distribution of below-normal events shows very low confidence. In such case, a reliability diagram based on equally populated bins of forecast probabilities is useful to improve the reliability analysis. The application of this technique to the below-normal events highlights residual resolution up to week 4 for very low probabilities. ROC diagrams for the same kind of events confirm that the modeling system has greater discrimination capability in case of below-normal events.

The reliability analysis is also performed for accumulated precipitation. The forecast skill is lower than T2m and only minor differences are observed between below- and above-normal precipitation.

Acknowledgments

The authors are grateful to the NCEP for providing forecast initialization data and to the ECMWF for providing reanalysis data. The CNR-ISAC subseasonal forecasting activity was partly supported by the Italian Civil Protection Agency.

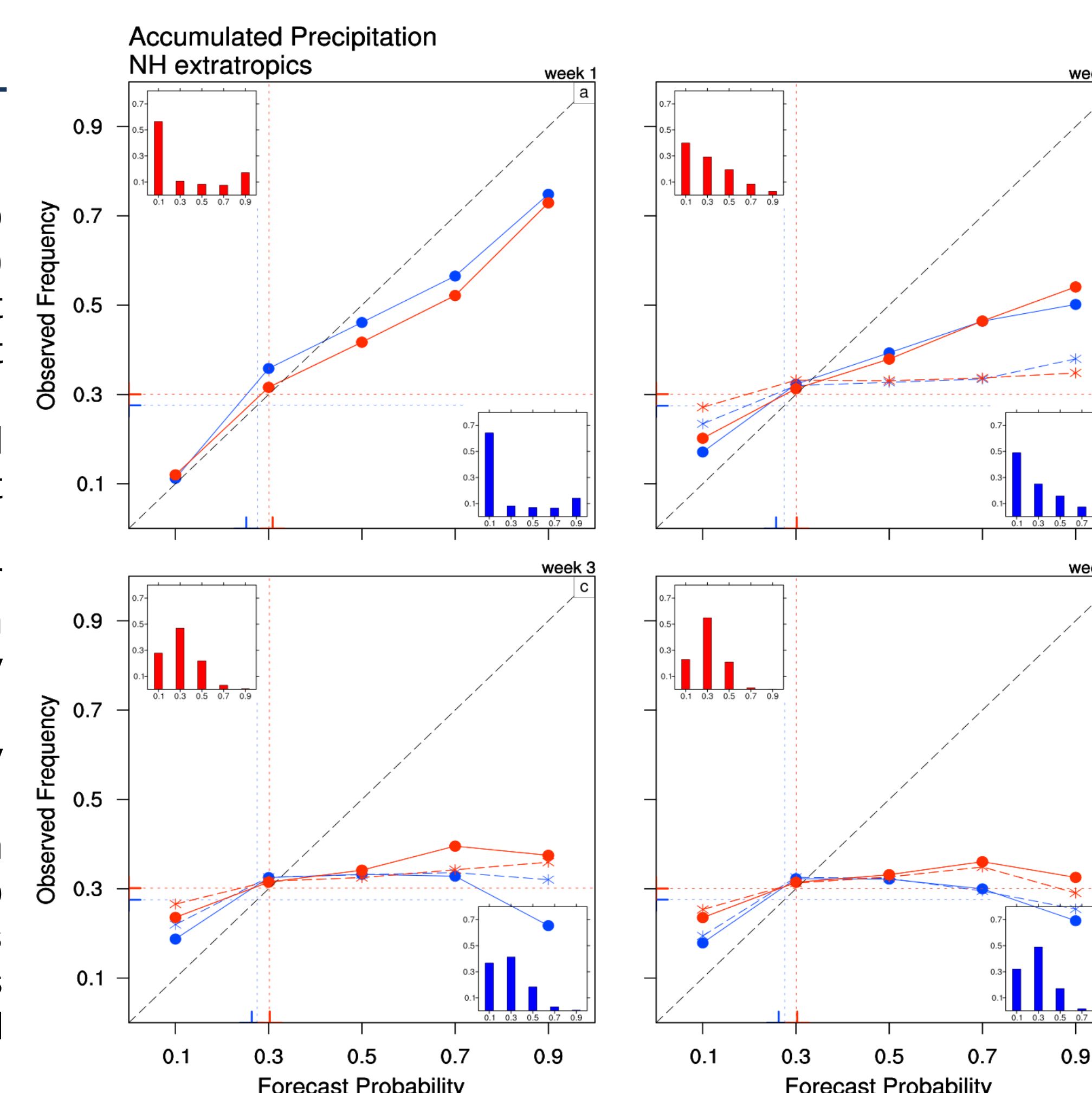


Fig.5: As in Fig. 2 but for below- and above-normal total accumulated precipitation